Charge-current generation in atomic systems induced by optical vortices

K. Köksal
Faculty of Arts and Science, Bitlis Eren University, 13000 Bitlis, Turkey and Institut für Physik, Martin-Luther-Universität Halle-Wittenberg, Heinrich-Damerow-Strasse 4, 06120 Halle, Germany

J. Berakdar
Institut für Physik, Martin-Luther-Universität Halle-Wittenberg, Heinrich-Damerow-Strasse 4, 06120 Halle, Germany
(Received 3 May 2012; published 11 December 2012)

We envisage the possibility of producing and tuning electronic orbital currents in atoms by weak, spatially inhomogeneous laser pulses with optical vortices. As already known, when interacting with such pulses an electronic system attains a definite amount of angular momentum. Here we explore this effect in the case when the system size is atomically small, i.e., much smaller than the scale of the inhomogeneity of the light pulses. We show that, nonetheless, angular momentum is transferred to the atomic system. The amount of the attained angular momentum depends on the position of the atom inside the field. Our numerical calculations and analytical analysis show that, indeed, light-induced orbital magnetism emerges in a dilute atomic gas when it is exposed to resonant or broadband optical vortices. This effect can be assessed, for instance, in a Faraday rotation experiment.

DOI: 10.1103/PhysRevA.86.063812 PACS number(s): 42.50.Tx, 32.30.−r, 32.10.Dk

I. INTRODUCTION

Currently, intensive research is devoted to the generation and control of magnetism via optical means with the promise of a wide range of applications, e.g., as detailed in Refs. [1–7]. The underlying microscopic mechanism for the observed effect of a moderate intensity laser field on the magnetic order, or on a local scale, on the spin dynamics is still under discussion. It is conceivable, however, that on the short, electronic time scale the laser's electric field would drive the electronic charge. This excitation is then mediated to the spin degrees of freedom via some sort of spin-orbital coupling. A direct Zeeman-type interaction of the magnetic-field component of the laser with the electrons' spins seems unlikely at the intensities considered experimentally so far [1–7].

Therefore, a desirable advance in this area would be the generation and the control of magnetic pulses that act directly on the sample magnetic order and trigger a magnetic dynamics and possibly a switching, similar to that recently realized and analyzed in Ref. [8]. In fact, this would enable a steering of the magnetization on a subpicosecond time scale [9]. One of the advantages of this procedure is the direct Zeeman-type coupling to the spin-degrees of freedom without the necessity for the (generally weak) spin-orbital interaction. Hence, the question arises of how to generate and spatiotemporally control magnetic fields. In essence this leads to the question of how to trigger and tune, on a desirable time scale, a charge current whose associated magnetic field can be utilized to probe the magnetic dynamics in a nearby sample. A practical option has been to combine the possibility of the precise temporal and polarization control of the plane-wave electromagnetic (EM) field [10] with the versatile possibilities of nanostructuring electronic confinement potentials. For example, currents can be generated in a quantum wire due to quantum interferences in one-photon, two-photon absorption [11] from a harmonic plane-wave EM pulse. Alternatively, we may drive directly a net current in the wire via an appropriate time structuring of the pulse [12]. This current may even be made dependent on the spin channel.

A further well-studied example is the light-induced generation of a current loop in a quantum ring [13,14]. The associated (orbital) magnetic dipole is then localized practically on the length scale set by the size of the ring (which can be fabricated to be even a few tens of nanometers [15]). The ultimate limit of the spatial localization would be to generate the currents within a single atom [16]; the localization of the atom itself is, however, another issue. A qualitatively different route is the spatial and temporal structuring of the light beam, as done, for example, with a laser beam carrying orbital angular momentum (OAM) as it occurs in an optical vortex [17–26] (sometimes this type of beam is also called twisted light). An example of the intensity profile of an OAM carrying beam in the plane perpendicular to the propagation direction is shown schematically in Fig. 1. The cylindrically symmetric intensity has a donut shape with a size set by the beam waist w_0. Over the past decade it has been established that OAM carrying beams are very instrumental for trapping and optical tweezers applications [17–25]. Charge currents may also be induced by these beams [27–30], and in the presence of spin-orbital coupling the spin degrees of freedom may also be accessed [30].

As is evident from Fig. 1, however, the extent of the generated magnetic field due to the orbital current is set by the laser spot, which is diffraction limited. One may consider the beam's self-focusing in nonlinear media [31]; however, the range in which the laser spot size can be tuned turned out to be limited. Hence, we are currently considering generating currents in nanosize systems, such as free or surface-deposited clusters, and here we report the analysis for simple atoms that should provide guidance for further studies on more involved targets. The interaction of an OAM carrying beam with atoms has been explored theoretically [32,33] with the prediction that, in principle, such a beam may result in a light-induced torque that can be exploited to control the atom's rotational motion. Furthermore, nondipolar electronic transitions may occur [32]. The effect of the OAM carrying beam on the atoms has also been discussed by Jáuregui [34] and van Enk [35], who discussed the internal and center-of-mass motion of the

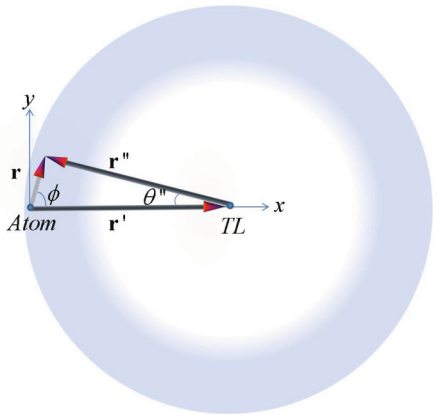

FIG. 1. (Color online) A schematic of the used notation. The vector $\mathbf{r}$ denotes the position of the electron with respect to the center of mass of the atom, while $\mathbf{r}''$ is the position of this electron with respect to the optical axis of the OAM carrying beam that propagates along the z axis. $\mathbf{r}' = \mathbf{r}'' - \mathbf{r}$ is the distance between the center of mass of the atom and the optical axis. The shaded circular area indicates schematically the region of high intensity.

atoms. Usually, the atomic orbitals and beam waist differ by orders of magnitudes, however. Thus, a practical realization is hindered by the fact that a huge laser intensity would be required to observe any influence of the beam on the atom when it resides on the optical axis, as can be anticipated from Fig. 1.

Moving the atom away from the optical axis, the symmetries of the atom and of the beam do not coincide, and one has to consider carefully the interplay of excitations due to the beam's radial and angular profiles. Experimentally, one may prepare the laser beam to intercept an atomic beam or to traverse a gas cell with the atoms distributed evenly on the beam spot. Geometrically, the atoms around the optical axis have a minor contribution to the attained properties of the gas cell. Hence, it is essential to analyze electronic excitations in atoms located off the optical axis. This is also important in view of generating localized orbital currents, e.g., in atoms physisorbed on a scanning tip, in which case the atoms would most probably not be positioned on the optical axis.

To keep the analysis as transparent as possible we consider in the next section an optical vortex with a low topological charge and zero radial nodes acting on a hydrogenic target. With the aim to induce nondestructively orbital current we focus on the case of single-photon transitions; i.e., the intensity-frequency ratio is small, and hence light-matter interaction can be treated perturbatively. In the following sections we present the analysis and the numerical illustrations for the dependence of electronic excitations on the atom's spatial position within the beam, with a special focus on current-carrying excited states. We find that, in addition to the beam's angular structure, the radial profile of the laser beam plays, in general, an important role. In general, we confirm the possibility of generating orbital currents in atoms with a low-intensity linearly polarized optical vortex despite the small extent of the atom with respect to the beam radial size and even if the atom is not on the optical axis.

II. THEORY

We consider a one-electron ion or atom interacting with an optical vortex, i.e., an inhomogeneous electromagnetic field that carries a topological charge. When interacting with such a beam, the system attains a definite amount of an orbital angular momentum (beyond that stemming for the light polarization, i.e., the photon spin). The vector potential $\mathbf{A}$ of a monochromatic light, e.g., as employed in this work has, in cylindrical coordinates, the form (the light propagates along the z direction)

$$\mathbf{A}(r'',\theta'',t) = \hat{\mathbf{e}} A_0 F^p_{m_a}(r'') e^{-i\omega t - \delta|t|} e^{iq_z z} + \text{c.c.} \qquad (1)$$

Here $\hat{\mathbf{e}} = (\cos\gamma, i\sin\gamma, 0)$ is the polarization vector with degree of ellipticity γ. A_0 is the amplitude of the vector potential. Throughout this work we use moderate intensities and high frequency ω such that the time-dependent perturbation theory with respect to the external field is applicable. The duration of the light pulse is quantified by the positive real parameter δ. q_z is the wave vector along the z axis. For the photon energies we are considering and for the size confinement of the electron with which the photons are interacting the usual dipole approximation with respect to the z direction is well justified and will be implicitly employed in the calculations below. The spatial structure of the beam in the x-y plane is described by the function $F^p_{m_a}$:

$$F^p_{m_a}(r'') = L_p^{|m_a|}\left(\frac{2r''^2}{w_0^2}\right) e^{-\frac{r''^2}{w_0^2}} \left(\frac{\sqrt{2}r''}{w_0}\right)^{|m_a|} e^{im_a\theta''}, \qquad (2)$$

where $m_a \in \mathbb{Z}$ is the topological charge of the optical vortex and $L_p^{|m_a|}$ is the associated Laguerre polynomial. Hence, m_a is related to the field angular structure, and p is the number of radial nodes of the intensity. w_0 is the waist of the beam.

Our aim is to study the interaction of one electron bound to a nuclear charge Z with $\mathbf{A}$. Neglecting terms of the order m_e/M, where m_e (M) is the electron (ion) mass; in the center-of-mass system of the atom the electronic wave function reads [we will use, in general, atomic units (a.u.) and refer in some places to other units conventionally used in experiments]

$$\begin{aligned}\psi_{n\ell m}(r,\theta,\phi) &= R_{n\ell}(r) Y_{\ell m}(\theta,\phi) \\ &= \sqrt{\left(\frac{2Z}{na_0}\right)^3 \frac{(n-\ell-1)!}{2n(n+\ell)!}} \left(\frac{2Zr}{na_0}\right)^{\ell} e^{-\frac{Zr}{na_0}} \\ &\quad \times L^{2\ell+1}_{n-\ell-1}\left(\frac{2Zr}{na_0}\right) \sqrt{\left(\frac{2\ell+1}{4\pi}\right)\frac{(\ell-m)!}{(\ell+m)!}} \\ &\quad \times P^m_\ell(\cos\theta) e^{im\phi}. \end{aligned} \qquad (3)$$

We use standard notation; that is, n, ℓ, and m are the principle, the orbital, and the magnetic quantum numbers, respectively, $R_{n\ell}$ is the radial function, $Y_{\ell m}(\theta,\phi)$ is spherical harmonics, and a_0 is the Bohr radius.

We are particularly interested in the following scenario: The waist of the beam w_0 is typically in the (sub)micron scale, whereas the extent of the atomic wave functions is typically orders of magnitudes smaller. This means that atoms residing at the center of the beam (i.e., for $\mathbf{r}' = 0$ in Fig. 1) or located well beyond w_0 (as seen from the center of the beam) are barely influenced by the light field. On the other hand, if the atom

happens to be at the intensity maximum of the field, it would feel only the local structure of the light field, which for this matter resembles a Gaussian beam. Hence, one may conclude that either the atom is not affected by the external field or the angular momentum transfer to the atom is associated with the spin of the photon and/or the spatial gradient of the local intensity profile. On the other hand, the topological charge m_a is associated with $\mathbf{A}$ as a whole, as is evident from Eq. (2), and is expected to be imprinted onto the electron motion once the photon is absorbed on a sub-Angstrom length scale, even though the spatial length scale of $\mathbf{A}$ (set by the wavelength) is orders of magnitude larger. It is our aim to quantify these issues analytically and with numerical simulations.

Starting from the classical Lagrangian within the minimal coupling, performing the Legendre transformation, and quantizing the matter field, we end up with the standard configuration-space form for the Hamiltonian [SI units are used, $V(r)$ is the spherically symmetric Coulomb potential, and $\hat{\mathbf{p}}$ is the electron momentum operator]

$$\hat{H} = \tfrac{1}{2}[\hat{\mathbf{p}} - \mathbf{A}(r'',\theta'',t)]^2 + V(r) + \Phi(\mathbf{r}'',t). \tag{4}$$

We note that $\mathbf{A}$ has both transversal and longitudinal components. The latter is of the order of q_z and can hence be neglected for the frequencies used in this work. We select a gauge in which the scalar potential $\Phi = 0$ and $\nabla_{\mathbf{r}''} \cdot \mathbf{A} = 0$ [this condition can be verified explicitly for Eq. (2)]. Hence, we can write Eq. (4) as $\hat{H} = \hat{H}_0 + \hat{H}_{1t}$, where $\hat{H}_0 = \hat{\mathbf{p}}^2/2 + V(r)$ and $\hat{H}_{1t} = -[\hat{\mathbf{p}} \cdot \mathbf{A}(r'',\theta'',t) + \mathbf{A}(r'',\theta'',t) \cdot \hat{\mathbf{p}}]/2$. The A^2 term has been neglected. Note that, due to the inhomogeneity of the vector potential, it is not obvious how to apply the Göppert-Mayer transformation that maps this velocity form of the electron-photon coupling to the length form. Below we show, however, how a structure of the matrix elements akin to the length form can still be retrieved.

To proceed further we expand the time-dependent wave function Ψ in terms of the normalized eigenfunction $\psi_k(\mathbf{r})$ of $\hat{H}_0$ with the eigenenergies E_n, i.e., $\Psi(\mathbf{r},t) = \sum_k C_k(t) e^{-i\omega_k t}\psi_k(\mathbf{r})$, where k is a collective quantum number referring to $\{n\ell m\}$ and $C_k(t)$ are the expansion coefficients. From the Schrödinger equation it follows that

$$i\dot{C}_k = -\sum_{k'} C_{k'} e^{i(\omega_k - \omega_{k'})t} e^{-i\omega t - \delta|t|} \langle k|H_1|k'\rangle + \text{c.c.}, \tag{5}$$

where $H_{1t} = H_1 e^{-i\omega t - \delta|t|}$. To a linear order in the field, i.e., considering single-photon processes, one finds in a standard way that

$$C_k \approx i\langle k|H_1|k_0\rangle \int_{-\infty}^{t_f} e^{i(\omega_k - \omega_{k_0} - \omega)t - \delta|t|} dt + \text{c.c.}, \tag{6}$$

where k_0 characterizes the state long before the field is switched on. We further write

$$C_k = i G_{k,k_0} \langle k|H_1|k_0\rangle, \tag{7}$$

with

$$G_{k,k_0} = -i\frac{e^{it_f(\omega_k - \omega_{k_0} - \omega + i\delta)}}{\omega_k - \omega_{k_0} - \omega + i\delta} + \frac{2\delta}{(\omega_k - \omega_{k_0} - \omega)^2 + \delta^2}. \tag{8}$$

For a long $t_f > 1/\delta$ this factor is the Fourier transform of the envelope function if $1/\delta$ is on the scale of the involved atomic transition times (which might well be the case when large-n states with small level spacings are participating). For a smooth temporal envelope on this time scale we obtain a δ function stating the energy conservation and leading to the standard Fermi's golden rule.

Of a particular interest for us is the photoinduced current that derives from the photoinduced current density (hereafter, unless explicitly stated, we use the abbreviation $\nabla_{\mathbf{r}} \equiv \nabla$):

$$\mathbf{j}(\mathbf{r}) = \frac{i}{2}[\Psi(\mathbf{r},t_f)\nabla\Psi^*(\mathbf{r},t_f) - \Psi^*(\mathbf{r},t_f)\nabla\Psi(\mathbf{r},t_f)], \tag{9}$$

which reads explicitly

$$\mathbf{j}(\mathbf{r}) = \frac{i}{2}\sum_k \sum_{k'} G_{k,k_0} G^*_{k',k_0} \langle k|H_1|k_0\rangle \langle k'|H_1|k_0\rangle^* \times e^{-i(\omega_k - \omega_{k'})t}(j_r\hat{\mathbf{r}} + j_\theta\hat{\boldsymbol{\theta}} + j_\phi\hat{\boldsymbol{\phi}}), \tag{10}$$

where j_r, j_θ, and j_ϕ govern the current densities in the radial, the orbital, and the azimuthal directions, respectively, and have the explicit forms

$$\begin{aligned} j_r &= N_{\ell,m} N_{\ell',m'} P_\ell^m(\cos\theta) P_{\ell'}^{m'}(\cos\theta) e^{im\phi} e^{im'\phi} \\ &\quad \times \left[R_{n,\ell}(r)\frac{\partial R_{n',\ell'}(r)}{\partial r} - R_{n',\ell'}(r)\frac{\partial R_{n,\ell}(r)}{\partial r} \right] \\ j_\theta &= N_{\ell,m} N_{\ell',m'} R_{n,\ell}(r) R_{n',\ell'}(r) e^{im\phi} e^{im'\phi} \\ &\quad \times \left[P_\ell^m(\cos\theta)\frac{\partial P_{\ell'}^{m'}(\cos\theta)}{r\partial\theta} - P_{\ell'}^{m'}(\cos\theta)\frac{\partial P_\ell^m(\cos\theta)}{r\partial\theta} \right]. \end{aligned} \tag{11}$$

The azimuthal current density is

$$j_\phi = -\frac{i(m+m')e^{i(m-m')\phi}}{r\sin\theta} N_{\ell,m} N_{\ell',m'} R_{n,\ell}(r) R_{n',\ell'}(r) \times P_\ell^m(\cos\theta) P_{\ell'}^{m'}(\cos\theta), \tag{12}$$

with the factor $N_{\ell,m} = \sqrt{\frac{2\ell+1}{4\pi}\frac{(\ell-m)!}{(\ell+m)!}}$. The current in azimuthal direction, given by

$$\mathbf{j}_\phi(\mathbf{r}) = -\sum_{n,\ell,m} m \left| G_{n\ell m,n_0\ell_0 m_0} M_{n\ell m,n_0\ell_0 m_0} \right|^2 \times \left(\frac{|\psi_{n,\ell,m}(r,\theta,\phi)|^2}{r\sin\theta} \right) \hat{\boldsymbol{\phi}}, \tag{13}$$

is the key factor for the orbital current, where $M_{n\ell m,n_0\ell_0 m_0} = \langle n\ell m|H_1|n_0\ell_0 m_0\rangle$. The induced current that we obtain by integrating Eq. (13) over $(\mathbf{r})$,

$$I_\phi = -\sum_{n,\ell,m} m \left| G_{n\ell m,n_0\ell_0 m_0} M_{n\ell m,n_0\ell_0 m_0} \right|^2 \times \int_0^\infty \int_0^\pi \frac{|\psi_{n,l,m}(r,\theta,\phi)|^2}{\sin\theta} d\theta\, dr\hat{\boldsymbol{\phi}}, \tag{14}$$

exposes the intimate relationship of the magnetic quantum number m and the probability to reach it as expressed by

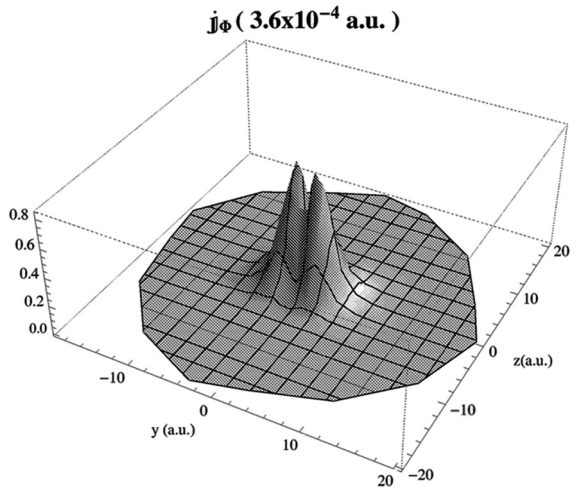

(a) $m_a = 0$

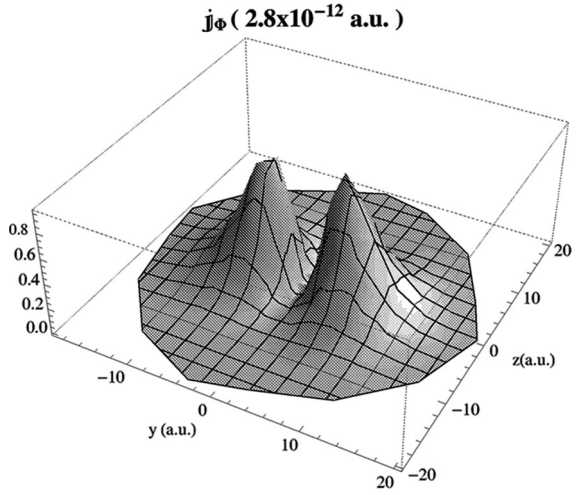

(b) $m_a = 1$

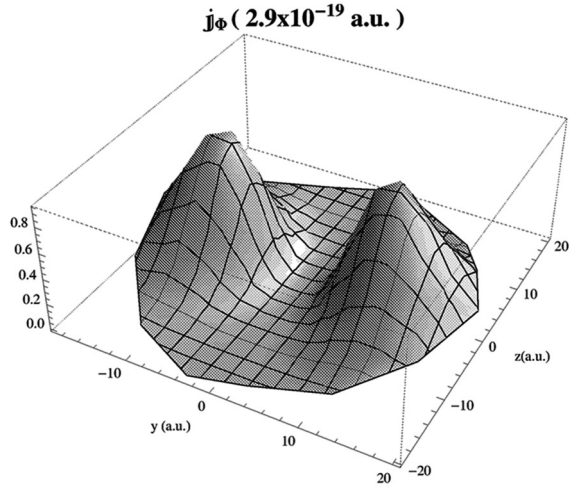

(c) $m_a = 2$

FIG. 2. The current density in a.u. as a function of $y = r\sin\theta$ and $z = r\cos\theta$ for different topological charges, for $\omega = 0.375$ a.u., and for $x = 0$. Other parameters are $\delta = 0.03$ a.u., the beam waist is 1.0×10^3 a.u., and the amplitude of the electric field is $A_0\omega = 0.03$ a.u.

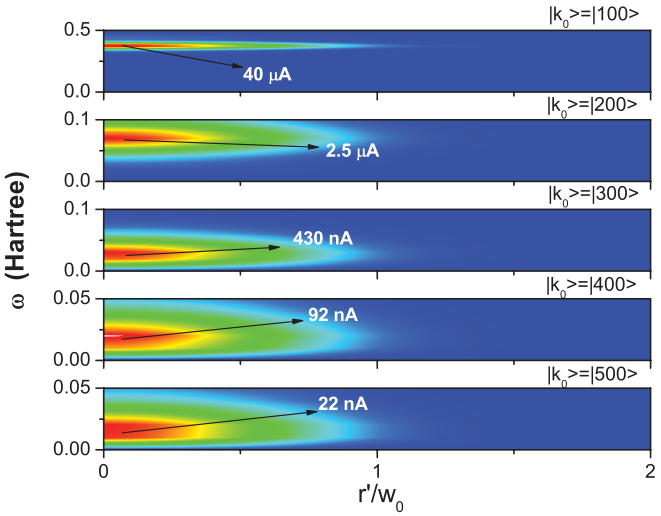

(a) First five initial states for $m_a = 0$

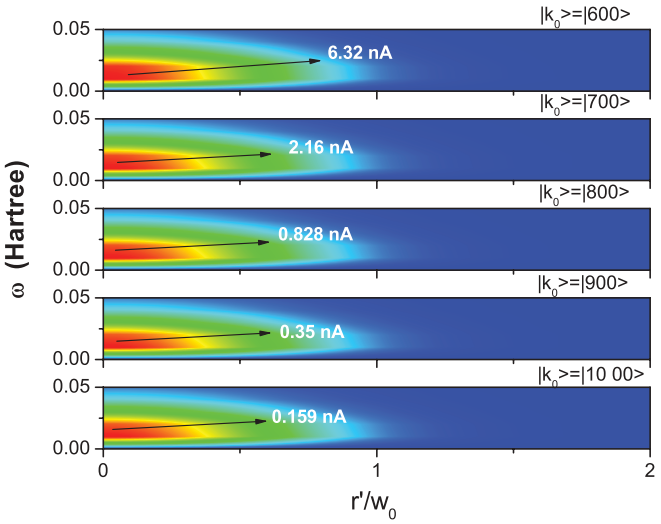

(b) Last five initial states for $m_a = 0$

FIG. 3. (Color online) The induced current as a function of the off-center shift parameter and of the frequency for a hydrogen atom. The light is circularly polarized with $m_a = 0$. We choose $\delta = 0.03$ a.u. and $t_f \to \infty$. The panels in (a) and (b) are obtained for different initial electronic states, as indicated upon each panel with the brackets $|k_0\rangle = |n_0\ell_0 m_0\rangle$. The dominant contributions to the current stem from the transitions to the levels $|(n_0+1)\ell m\rangle \cdots |(n_0+5)\ell m\rangle$.

the associated transition matrix elements. For short pulses the spectral width of the pulse (encapsulated in G) may cover several of these transitions.

Let us inspect now the structure of the transition matrix elements

$$M_{k,k_0} = \langle k|(\nabla\cdot\mathbf{A} + \mathbf{A}\cdot\nabla + \mathbf{A}\cdot\nabla)|k_0\rangle/2; \qquad (15)$$

we note that because $\nabla\cdot\mathbf{A} = 0$, it follows that $(\mathbf{A}\cdot\hat{\mathbf{p}})\psi = \hat{\mathbf{p}}\cdot\mathbf{A}\psi$ (where ψ is an arbitrary wave function) and hence $\mathbf{A}$ commutes also with the atomic Hamiltonian $\hat{H}_0$. Since $\hat{\mathbf{p}} = -i[\hat{\mathbf{r}}, \hat{H}_0]$, we infer the length-type form of the matrix elements (15),

$$M_{n\ell m,n_0\ell_0 m_0} = \langle n\ell m|\hat{H}_0|n\ell m\rangle\langle n\ell m|\mathbf{A}\cdot\mathbf{r}|n_0\ell_0 m_0\rangle - \langle n\ell m|\mathbf{A}\cdot\mathbf{r}|n_0\ell_0 m_0\rangle\langle n_0\ell_0 m_0|\hat{H}_0|n_0\ell_0 m_0\rangle$$

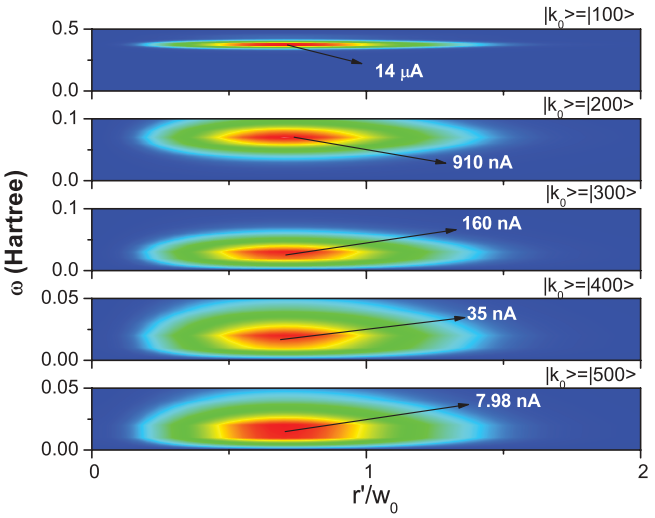

(a) First five initial states for $m_a = 1$

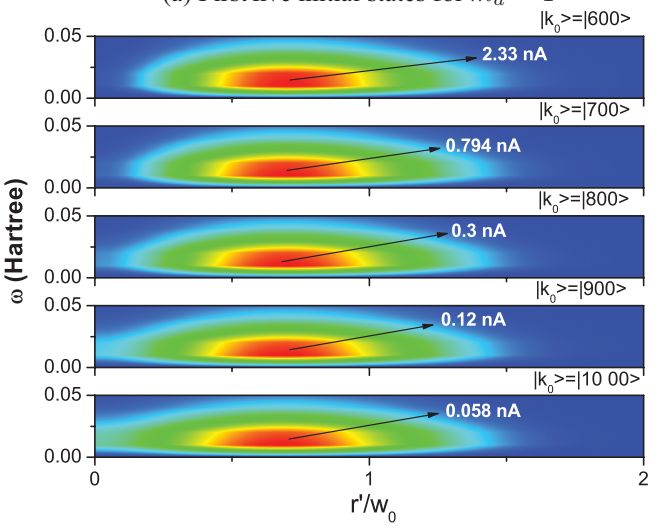

(b) Last five initial states for $m_a = 1$

FIG. 4. (Color online) The induced current as a function of the off-center shift parameter and of the frequency for a hydrogen atom. The light is circularly polarized with $m_a = 1$ and $\delta = 0.03$ a.u. and $t_f \to \infty$. The panels in (a) and (b) are obtained for different initial electronic states, as indicated upon each panel with the brackets $|k_0\rangle = |n_0\ell_0 m_0\rangle$. The dominant contributions to the current stem from the transitions to the levels $|(n_0+1)\ell m\rangle \cdots |(n_0+5)\ell m\rangle$.

$$
\begin{aligned}
&= -i\left(E_{n\ell m} - E_{n_0\ell_0 m_0}\right)\langle n\ell m|\mathbf{A}\cdot\mathbf{r}|n_0\ell_0 m_0\rangle \\
&= -i\left(E_{n\ell m} - E_{n_0\ell_0 m_0}\right)A_0\langle n\ell m|F^p_{m_a}(r'')e^{im_a\theta''} \\
&\quad \times \hat{\mathbf{e}}\cdot\mathbf{r}|n_0\ell_0 m_0\rangle \\
&= -i\left(E_{n\ell m} - E_{n_0\ell_0 m_0}\right)A_0\langle n\ell m|F^p_{m_a}(r'')e^{im_a\theta''} \\
&\quad \times r\sin\theta(\cos\gamma\cos\phi + i\sin\gamma\sin\phi)|n_0\ell_0 m_0\rangle.
\end{aligned}
\tag{16}
$$

Here we skip further standard technicalities. For details on the time-dependent perturbation theory we refer to Refs. [36,37]. Aspects of the photoinduced current using different formalisms can be found in the studies of Hebborn and March [38], Wood and Ashcroft [39] and Keller and Wang [40,41].

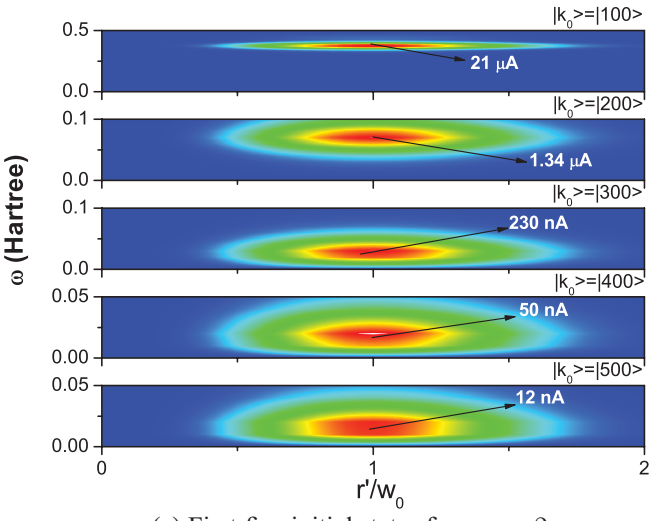

(a) First five initial states for $m_a = 2$

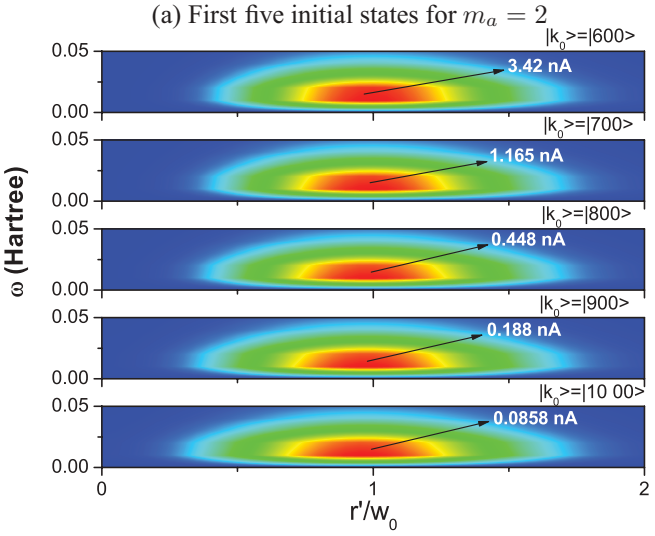

(b) Last five initial states for $m_a = 2$

FIG. 5. (Color online) The induced current as a function of the off-center shift parameter and of the frequency for a hydrogen atom. The light is circularly polarized with $m_a = 2$. We choose $\delta = 0.03$ a.u. and $t_f \to \infty$. The panels in (a) and (b) are obtained for different initial electronic states, as indicated upon each panel with the brackets $|k_0\rangle = |n_0\ell_0 m_0\rangle$. The dominant contributions to the current stem from the transitions to the levels $|(n_0+1)\ell m\rangle \cdots |(n_0+5)\ell m\rangle$.

III. ATOMS IN THE CENTER OF AN OAM CARRYING BEAM

Photoinduced currents in atomic systems using spatially homogeneous laser pulses have been considered by Barth *et al.* [16]. Currents in atoms with laser pulses carrying angular momentum were considered in Ref. [32]. However, if the atoms reside at the center of the optical beam axis (where the light intensity is extremely small), a sizable atomic excitation occurs only at extremely large laser intensities (the theory was still performed nonrelativistically, however). Here, we consider therefore an ensemble of atoms distributed evenly over the laser spot. The atoms residing at the optical axis (i.e., for $\mathbf{r}' = 0$ in Fig. 1) are exposed to a very low light intensity, compared to the peak-field intensity. In addition, geometrically, these atoms have, however, a small relative

proportion compared to the whole atomic ensemble. Thus, it is of interest to trace the type of atomic excitations as we move the atom off the optical axis.

For clarity we briefly discuss the case of $\mathbf{r}' = 0$, choosing $p = 0$ for the radial node. Other choices do not create qualitatively new problems.

For a circularly polarized light $\gamma = \pi/4$ with a frequency resonant with the $E_{100} \longmapsto E_{2\ell m}$ transition one finds for the matrix element from Eq. (16) that if $m_a = 0$, then as expected (note that the spatial envelop is included here, however), $M_{200,100} = M_{210,100} = M_{100,100} = 0$, and

$$M_{21\pm1,100} = \pm i \frac{A_0}{\sqrt{2}}(E_{21\pm1} - E_{100})\,\frac{256}{243}, \tag{17}$$

where $\pm$ stand for right and left circularly polarized light, respectively (right and left are defined in the sense that the electric-field vector of the light rotates clockwise and anticlockwise when viewed along the beam propagation). The induced current density follows from Eqs. (12) and (13) as

$$\mathbf{j}_\phi(r,\theta) = \mp\frac{A_0^2}{2}(E_{21\pm1} - E_{100})^2 \left(\frac{256}{243}\right)^2 \times G_{100,21\pm1}G^*_{100,21\pm1}\left(\frac{r^2 e^{-r}\sin^2\theta}{64\pi r\sin\theta}\right)\hat{\boldsymbol{\phi}}, \tag{18}$$

and the induced current is thus

$$I_\phi = -\frac{A_0^2}{16\pi}\frac{(E_{21\pm1} - E_{100})^2}{2}\left(\frac{256}{243}\right)^2 [G_{100,21\pm1}G^*_{100,21\pm1}]\hat{\boldsymbol{\phi}}, \tag{19}$$

where $G_{100,21\pm1}$ includes the pulse temporal parameters t_f and $1/\delta$ and the carrier frequency ω.

For an estimate of the current, let us take a pulse duration $\tau = 1/\delta = 372$ a.u. ≈ 9 fs, a carrier frequency of $\omega = 0.375$ a.u., and an electric-field amplitude $A_0\omega = 0.03$ a.u. We find then that the peak value of the induced current is 20.5 μA (recall, 1 a.u. of the current corresponds to $\approx$6.6 mA).

Figure 2 shows the current density in the x-y plane for $t_f \to \infty, \omega = 0.375$ a.u., $\delta = 0.03$ a.u. and for different values of m_a. The current density diminishes with increasing m_a because in this case the light intensity is pushed off the center of the optical axis where the atom is residing.

IV. ATOMS IN OFF-CENTER OAM CARRYING BEAMS

We consider now the atom irradiated by a focused Laguerre-Gaussian light beam. The atom may be located at an arbitrary position with respect to the optical axis. Due to symmetry it suffices to consider the variation in the atomic excitations while shifting the center of mass of the atom along the x axis, i.e., by varying r', as depicted in Fig. 1.

A. An analytical treatment for $m_a = 0$ and nondipolar contributions

The shift of the LG beam gives rise to a new kind of transition in the case of linearly and circularly polarized laser beams. Note that there is an additional effect when we scan the atom through the spatial profile of the laser beam. Irrespective of the value of m_a, the pulse spatial profile may give rise to nondipolar transitions, especially for extended initial states. For a given initial state the largest effect is found at the point of steepest descent of the spatial profile. For instance, let us consider the case $m_a = p = 0$; the spatial structure of the LG beam reduces to a Gaussian one,

$$F_0^0(r'')e^{-i0\theta''} = e^{-\frac{r''^2}{w_0^2}}, \tag{20}$$

where $r''^2 = r^2 + r'^2 + 2rr'\cos\phi$. Then, if any, the strongest nondipolar transitions at low frequency are achieved when the atom resides in the region of steepest profile change around $r' = w_0/\sqrt{2}$. The change in the dipolar selection rules ($\Delta m = 0$ and $\Delta\ell = \pm1$ for linear polarization and $\Delta m = \pm1$ and $\Delta\ell = \pm\Delta m$ for circular polarization) due to the Gaussian spatial profile, Eq. (20), follows from an inspection of the matrix elements as r' increases. We find then that

$$\begin{aligned}
M &= e^{-\frac{r'^2}{w_0^2}}\left\{\sum_{j=0}^{\infty}\mathcal{L}_j\left(\frac{r}{w_0^2}\right)^j\sum_{k=-j}^{j}\mathcal{M}_k\beta\,\delta_{m,m_0\pm1+k}\sum_{\chi=0}^{\infty}\mathcal{N}_\chi[1-\delta_{k,0}(1-\delta_{\chi,1})]\rho\,\delta_{\ell,\ell_0+\chi}\right\} \quad \text{for} \quad \gamma = 0,\\
M &= e^{-\frac{r'^2}{w_0^2}}\left\{\sum_{j=0}^{\infty}\mathcal{L}_j\left(\frac{r}{w_0^2}\right)^j\sum_{k=-j}^{j}\mathcal{M}_k\beta\,\delta_{m,m_0+1+k}\sum_{\chi=0}^{\infty}\mathcal{N}_\chi[1-\delta_{k,0}(1-\delta_{\chi,1})]\rho\,\delta_{\ell,\ell_0+\chi}\right\} \quad \text{for} \quad \gamma = +45^\circ,\\
M &= e^{-\frac{r'^2}{w_0^2}}\left\{\sum_{j=0}^{\infty}\mathcal{L}_j\left(\frac{r}{w_0^2}\right)^j\sum_{k=-j}^{j}\mathcal{M}_k\beta\,\delta_{m,m_0-1+k}\sum_{\chi=0}^{\infty}\mathcal{N}_\chi[1-\delta_{k,0}(1-\delta_{\chi,1})]\rho\,\delta_{\ell,\ell_0+\chi}\right\} \quad \text{for} \quad \gamma = -45^\circ.
\end{aligned} \tag{21}$$

Here $\mathcal{L}_j$, $\mathcal{M}_k$, and $\mathcal{N}_\chi$ are the results of the radial, azimuthal, and orbital integrations, respectively. $\beta = \frac{(-1)^{k+\epsilon+1}+1}{2}$, $\rho = \frac{(-1)^{k+\chi+1}+1}{2}$, and $\epsilon = 2^{\frac{(-1)^j+1}{2}} - 1$. Obviously, nondipolar contributions develop as soon as the center of mass of the atom is shifted away from the optical axis, in which case the dipolar contribution decreases.

We also investigated the dependence of the magnitude of the transition matrix elements involving states $|15\ 00\rangle$ and $|16\ \ell m\rangle$ as a function of the shift parameter r' (in units of w_0). As explained above, the largest nondipolar contributions are expected to occur around the region of steepest decent of the spatial profile, which corresponds to $r' = w_0/\sqrt{2}$. This amounts to $r'/w_0 \approx 0.7$, which is nicely confirmed by the full

numerical calculations. Such an effect of the spatial profile variation has indeed been verified experimentally by Wells *et al.* [42].

B. Photoinduced charge current in off-center atoms due to a Laguerre-Gaussian laser beam

We inspect the induced current as a function of the off-center shift r', the topological charge, and the frequency of the laser beam. The parameters used for the calculation are $w_0 = 10^3$ a.u., $A_0 = 0.03$ a.u., $m_a = 0, 1,$ or 2, $p = 0$, and $\delta = 0.03$ a.u. The induced current is calculated according to Eq. (14).

The general expectation is that a linearly polarized light with $m_a = 0$ does not generate a net current. If the temporal profile is very short (in the sense detailed above), a nonequilibrium charge polarization (involving states with frequencies within the bandwidth of the pulse) is created in much the same way as the pulse-driven phase-coherent semiconductor-based quantum rings that we studied in full detail in Ref. [43]. Also from these studies we expect to induce a current by two time-delayed, phase-shifted linearly polarized pulses with orthogonal polarizations (cf. Ref. [13] and references therein). The generation of the current due to the nonhomogeneous spatial profile of a linear polarized pulse with $m_a = 0$ is, in principle, possible, e.g., by introducing directional angular modulations in the profile; in our case, however, such a current should be negligible.

For a finite m_a we expect, in general, the generation of a current since particles attain a definite amount of angular momentum related to m_a when interacting with such a pulse. As mentioned in the Introduction, this seems physically obvious for systems with an extent comparable to or larger than the pulse spot (in the latter case one expects to steer a local current in the system). For atomic systems with an average size well below w_0, the situation is not clear.

Figures 3–5 show the induced current as a function of the frequency and the off-center shift r' for different topological charges and different initial states. For the initial state $|n_0\ell_0 m_0\rangle = |100\rangle$, the topological charge $m_a = 0$, as can be seen from the first panel in Fig. 3(a), and the maximum value of the induced current is observed for $r' = 0$ and $\omega = 0.375$ a.u., which is the difference between the first and the second energy states, meaning that the largest contribution to the current is provided by dipole transitions to the next-nearest energy level. The maximal current is approximately 40 μA.

In Fig. 3(a), when the initial state of the electron is chosen to be $|n_0\ell_0 m_0\rangle = |200\rangle$, as in the second panel, the maximal current becomes 2.5 μA at $\omega = 0.07$ a.u. Pumping first to an excited initial state away from the ground state, the level spacing of the participating states decreases, and therefore we observe a shift of the peak current in Fig. 3 to lower frequencies

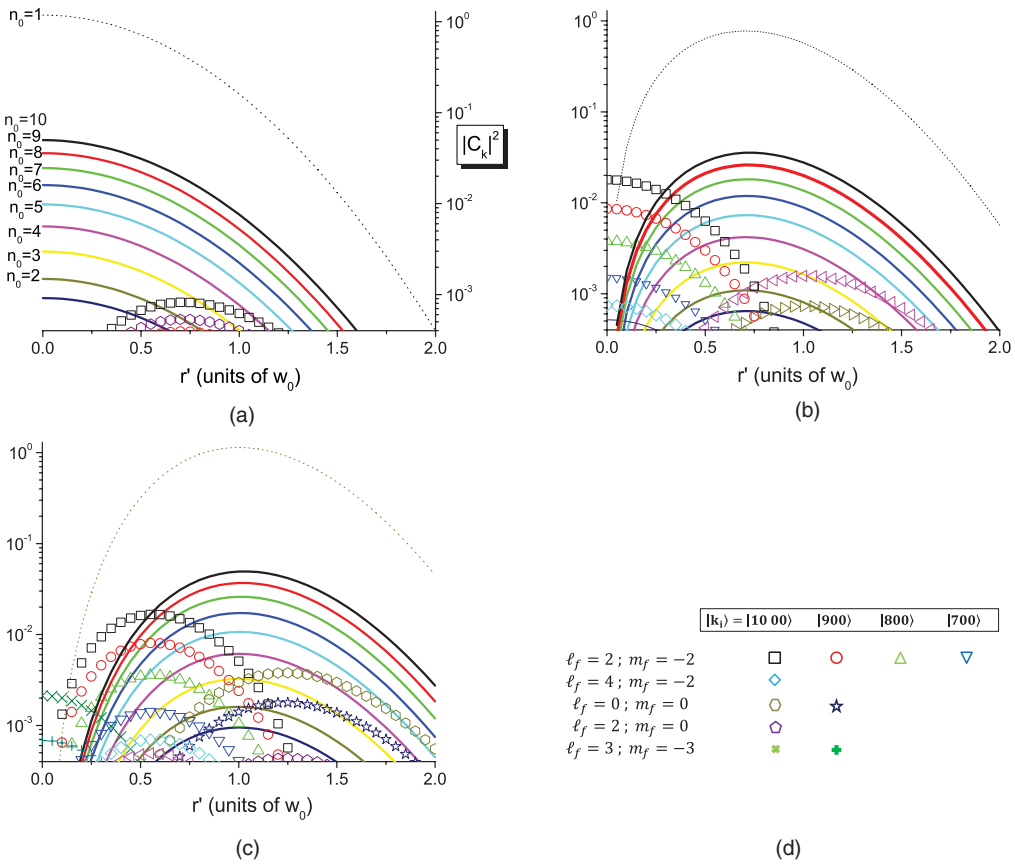

FIG. 6. (Color online) In the case of a circularly polarized laser beam, the contributions of the different transitions to the induced current as a function of the shifting parameter for (a) $m_a = 0$, (b) $m_a = 1$, and (c) $m_a = 2$. The subscript f indicates the final state. $n_0 = 1$ states are given by dashed lines, and $n_0 > 1$ states are shown by solid lines for $\ell_f = 1; m_f = -1$. The symbols indicate the nondipolar transitions.

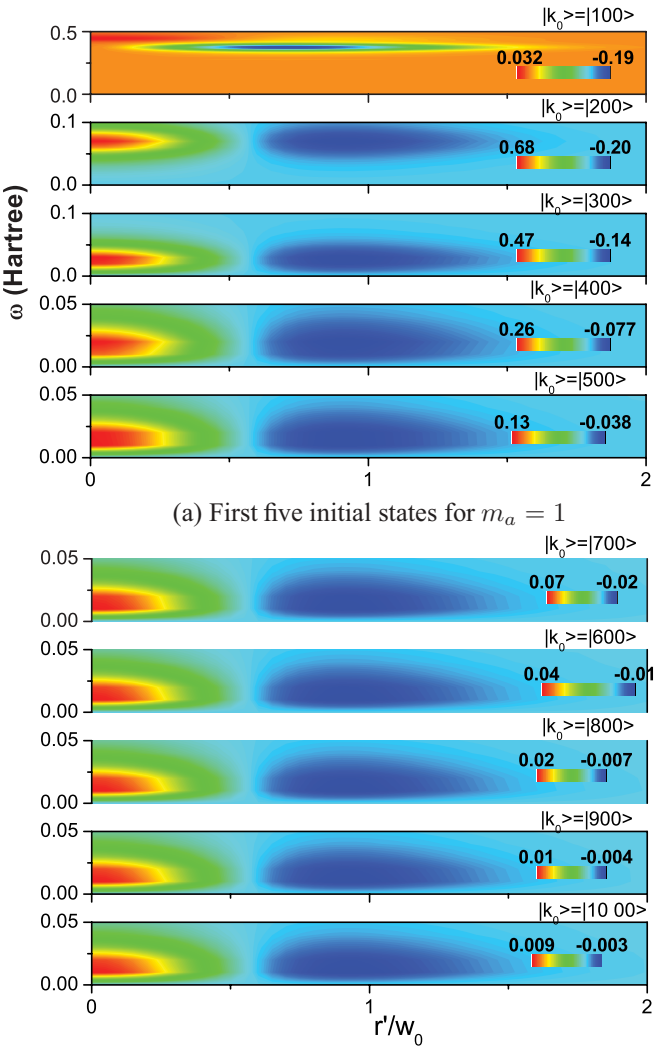

(a) First five initial states for $m_a = 1$

(b) Last five initial states for $m_a = 1$

FIG. 7. (Color online) The induced current in a hydrogen atom as a function of the off-center shift parameter and the frequency of a linearly polarized light for $m_a = 1$. No sizable current can be generated if $m_a = 0$. The beam duration is quantified by $\delta = 0.03$ a.u. and $t_f \to \infty$. (a) and (b) show the dependence on the initial states, as indicated on each panel with the brackets $|k_0\rangle = |n_0\ell_0 m_0\rangle$. The magnitude of the current as depicted on the panels is measured in units of nA.

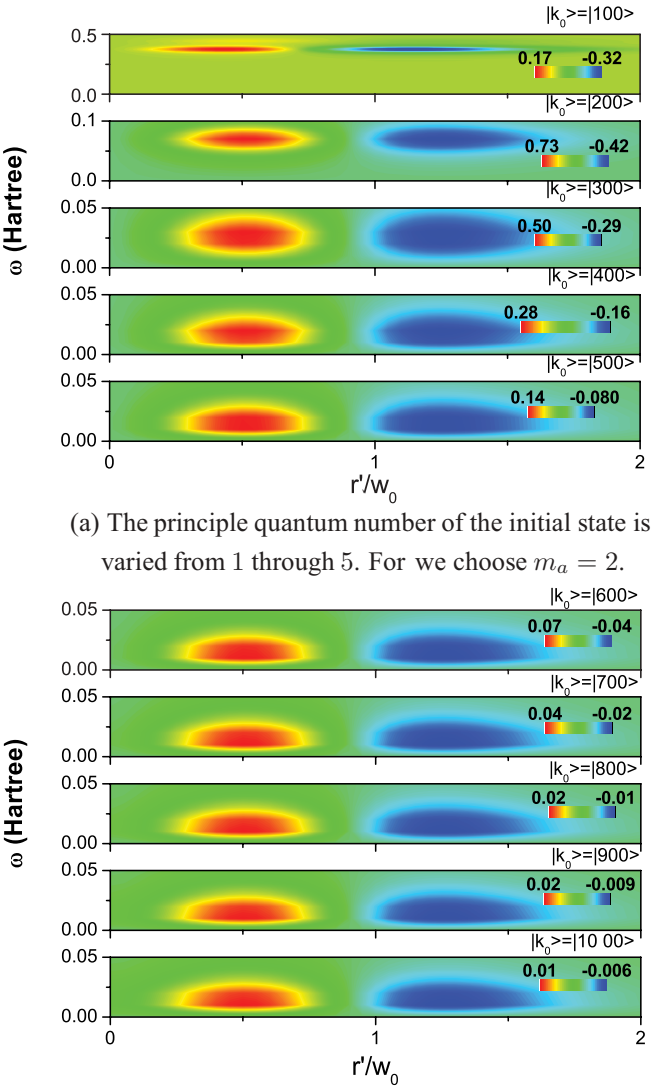

(a) The principle quantum number of the initial state is varied from 1 through 5. For we choose $m_a = 2$.

(b) The principle quantum number of the initial state is varied from 6 through 10 while $m_a = 2$.

FIG. 8. (Color online) The induced current in a hydrogen atom as a function of the off-center shift parameter and the frequency of a linearly polarized light for $m_a = 2$. The beam duration is quantified by $\delta = 0.03$ a.u. and $t_f \to \infty$. (a) and (b) show the dependence on the initial states, which are indicated on each panel with the brackets $|k_0\rangle = |n_0\ell_0 m_0\rangle$. The magnitude of the current as indicated on the panels is measured in units of nA.

of the light. The relative weight of the current carrying states is lower, and hence the current becomes weaker.

For $m_a = 1$ and $m_a = 2$ we expect the maximal current to emerge around the value $r' = w_0/\sqrt{2}$, as explained above, which is confirmed by the full numerical calculations. We notice here that a pulse with $m_a = 0$ generates more current than a pulse with $m_a = 1$ or $m_a = 2$, which seems counterintuitive. The explanation is, however, quite simple: The magnitude of vector potential (1) with $m_a = 1$ or $m_a = 2$ at the peak induced current ($r' \approx w_0/\sqrt{2}$) in Fig. 6(b) is smaller than the magnitude of vector potential (1) with $m_a = 0$ at $r' = 0$.

A comprehensive analysis is offered by the population probabilities $|C_k|^2$ of states $|k\rangle$, as shown by Fig. 6. The coefficient C_k is calculated according to Eq. (7). As an example we choose $\omega = 0.375$ a.u. and $\delta = 0.03$ a.u. As can be seen from Fig. 6(a), the most important contributions stem from the dipole transition for which $\Delta\ell = 1$ and $m_f - m_i = -1$ apply. For $m_a = 0$ the contributions are maximal when the atom is in the center of the beam (where the intensity is maximal) and decrease with increasing r'. Moving the atom across the beam profile, nondipolar contributions emerge and exhibit peak values around the position of steepest decent of the spatial profile of the beam (i.e., $r'/w_0 \approx 0.7$), as explained above. These transitions are governed by $\Delta\ell = 2$; $\Delta m = -2$ and $\Delta\ell = 0$; $\Delta m = 0$ for $n_f = 10$. As noted above, the spatial profile of the beam cannot induce angular currents.

The nondipolar transitions can be more effective in the case of $m_a = 1$ and $m_a = 2$. As can be seen from Figs. 6(b)

and 6(c), the number of new transitions increases if $m_a > 0$. Furthermore, for $r' = 0$ the magnitude of the nondipolar transitions is substantial and overwhelms the dipolar transitions in this case. Inspecting the induced current for $n_i > 8$ and $m_a > 0$ in Figs. 4 and 5, one observes an increase in the induced current when the off-center shift parameter is around zero. As can be seen from Fig. 1, the effect of m_a diminishes if $w_0 \gg \langle r \rangle$.

A linearly polarized Laguerre-Gaussian beam can induce a charge current if $m_a > 0$. Indeed, we confirmed numerically that the current diminishes if $m_a = 0$ (irrespective of r'). We employ the same parameters that we used in the calculations for the circular polarization case. As inferred from Figs. 7 and 8, an induced charge current emerges even for the case of a tightly confined orbitals, i.e., low principle quantum number. The magnitude of the current is in the nA range. Also note that the induced current changes sign and hence the direction when scanning r' for some initial states. The magnitudes of the positive and negative currents are, however, quite different. Hence, in an ensemble of atoms the resultant current should be observable.

V. CONCLUSIONS

We studied theoretically the effect of the structure of the spatial profile of a laser beam on the electronic transitions in a hydrogenic atom with a special focus on the possibility of inducing a charge current. Throughout the calculations, first-order time-dependent perturbation theory has been used. Analytical results have been obtained for a Gaussian profile showing that no current can be generated if the pulse is linearly polarized, even though nondipolar transitions may well be induced. For a light carrying angular momentum we find a finite current at moderate intensities and for both linear and circular polarizations. The magnitude of the current depends on the spatial position of the atom in the beam. Quantifying this dependence analytically and with numerical calculations, we conclude that for an ensemble of atoms distributed over the spot of the laser beam a finite charge current should be generated in the perturbative regime of the light-matter interaction. This offers a convenient tool for a light-induced orbital magnetism that can be tested, e.g., by measuring the Faraday rotation angle of the polarization plane of a traversing plane wave of light.

ACKNOWLEDGMENTS

We thank A. Thakur, Y. Pavlyukh, and A.S. Moskalenko for fruitful discussions. This work is supported by the DAAD and the DFG through Grant No. SFB 762.

[1] A. V. Kimel, A. Kirilyuk, and T. Rasing, Rev. Mod. Phys. **82**, 2731 (2010).

[2] J.-Y. Bigot, M. Vomir, and E. Beaurepaire, Nat. Phys. **5**, 515 (2009); G. P. Zhang, W. Hübner, G. Lefkidis, Y. Bai, and T. F. George, *ibid.* **5**, 499 (2009).

[3] A. V. Kimel, A. Kirilyuk, F. Hansteen, R. V. Pisarev, and T. Rasing, J. Phys. Condens. Matter **19**, 043201 (2007), and references therein.

[4] A. Melnikov, I. Razdolski, T. O. Wehling, E. Th. Papaioannou, V. Roddatis, P. Fumagalli, O. Aktsipetrov, A. I. Lichtenstein, and U. Bovensiepen, Phys. Rev. Lett. **107**, 076601 (2011).

[5] J. A. de Jong, A. V. Kimel, R. V. Pisarev, A. Kirilyuk, and Th. Rasing, Phys. Rev. B **84**, 104421 (2011).

[6] I. Radu, K. Vahaplar, C. Stamm, T. Kachel, N. Pontius, H. A. Dürr, T. A. Ostler, J. Barker, R. F. L. Evans, and R. W. Chantrell, Nature (London) **472**, 205 (2011).

[7] N. Kanda, T. Higuchi, H. Shimizu, K. Konishi, K. Yoshioka, and M. Kuwata-Gonokami, Nat. Commun. **2**, 362 (2011).

[8] S. Loth, M. Etzkorn, C. P. Lutz, D. M. Eigler, and A. J. Heinrich, Science **329**, 1628 (2010); S. Loth, S. Baumann, C. P. Lutz, D. M. Eigler, and A. J. Heinrich, *ibid.* **335**, 196 (2012); M. Schüler, Y. Pavlyukh, and J. Berakdar, New J. Phys. **14**, 043027 (2012).

[9] A. Sukhov and J. Berakdar, Phys. Rev. Lett. **102**, 057204 (2009); Phys. Rev. B **79**, 134433 (2009); Appl. Phys. A **98**, 837 (2010).

[10] A. M. Weiner, Rev. Sci. Instrum. **71**, 1929 (2000); T. Brixner and G. Gerber, Opt. Lett. **26**, 557 (2001); T. Brixner, Appl. Phys. B **76**, 531 (2003); L. Polachek, D. Oron, and Y. Silberberg, Opt. Lett. **31**, 631 (2006); F. Krausz and M. Ivanov, Rev. Mod. Phys. **81**, 163 (2009); U. Eichmann, T. Nubbemeyer, H. Rottke, and W. Sandner, Nature (London) **461**, 1261 (2009); M. Wollenhaupt and T. Baumert, Faraday Discuss. **153**, 9 (2011); B. Pearson and T. Weinacht, Nat. Photonics **6**, 78 (2012); E. Goulielmakis, *ibid.* **6**, 142 (2012); G. Sansone, F. Kelkensberg, F. Morales, J. F. Perez-Torres, F. Martín, and M. J. J. Vrakking, IEEE J. Sel. Top. Quantum Electron. **18**, 520 (2012); G. Sansone, F. Calegari, and M. Nisoli, *ibid.* **18**, 507 (2011); H. T. Nembach and T. J. Silva, Phys. Rev. X **2**, 011005 (2012).

[11] E. Dupont, P. B. Corkum, H. C. Liu, M. Buchanan, and Z. R. Wasilewski, Phys. Rev. Lett. **74**, 3596 (1995); H. M. van Driel, J. E. Sipe, and A. L. Smirl, Phys. Status Solidi B **243**, 2278 (2006); C. Ruppert, S. Thunich, G. Abstreiter, A. Fontcuberta i Morral, A. W. Holleitner, and M. Betz, Nano Lett. **10**, 1799 (2010).

[12] Z.-G. Zhu, C.-L. Jia, and J. Berakdar, Phys. Rev. B **82**, 235304 (2010).

[13] A. Matos-Abiague and J. Berakdar, Phys. Rev. Lett. **94**, 166801 (2005); Europhys. Lett. **69**, 277 (2005); A. S. Moskalenko, A. Matos-Abiague, and J. Berakdar, Phys. Rev. B **74**, 161303(R) (2006); A. S. Moskalenko and J. Berakdar, *ibid.* **80**, 193407 (2009); N. F. Hinsche, A. S. Moskalenko, and J. Berakdar, Phys. Rev. A **79**, 023822 (2009); Z.-G. Zhu and J. Berakdar, Phys. Rev. B **77**, 235438 (2008); J. Phys. Condens. Matter **21**, 145801 (2009).

[14] V. E. Kravtsov and V. I. Yudson, Phys. Rev. Lett. **70**, 210 (1993); P. Kopietz and A. Völker, Eur. Phys. J. B **3**, 397 (1998); M. Moskalets and M. Büttiker, Phys. Rev. B **66**, 245321 (2002); Y. V. Pershin and C. Piermarocchi, *ibid.* **72**, 245331 (2005); L. I. Magarill and A. V. Chaplik, JETP Lett. **70**, 615 (1999); K. Nobusada and K. Yabana, Phys. Rev. A **75**, 032518 (2007); E. Räsänen, A. Castro, J. Werschnik, A. Rubio, and E. K. U. Gross, Phys. Rev. Lett. **98**, 157404 (2007).

[15] A. Lorke, R. J. Luyken, A. O. Govorov, J. P. Kotthaus, J. M. Garcia, and P. M. Petroff, Phys. Rev. Lett. **84**, 2223 (2000);

W. Rabaud, L. Saminadayar, D. Mailly, K. Hasselbach, A. Benoit, and B. Etienne, *ibid.* **86**, 3124 (2001); A. Fuhrer *et al.*, Nature (London) **413**, 822 (2001).

[16] I. Barth *et al.*, J. Am. Chem. Soc. **128**, 7043 (2006); Angew. Chem., Int. Ed. **45**, 2962 (2006); I. Barth and J. Manz, in *Progress in Ultrafast Intense Laser Science VI*, Springer Series in Chemical Physics Vol. 99, edited by K. Yamanouchi, G. Gerber, A. D. Bandrauk, F. Schäfer, J. Toennies, and W. Zinth (Springer, Berlin, 2010), p. 2144, and references therein.

[17] V. Y. Bazhenov, M. V. Vasnetsov, and M. S. Soskin, JETP Lett. **52**, 429 (1990).

[18] L. Allen, M. W. Beijersbergen, R. J. C. Spreeuw, and J. P. Woerdman, Phys. Rev. A **45**, 8185 (1992).

[19] M. W. Beijersbergen, L. Allen, H. van der Veen, and J. P. Woerdman, Opt. Commun. **96**, 123 (1993).

[20] M. W. Beijersbergen, R. P. C. Coerwinkel, M. Kristensen, and J. P. Woerdman, Opt. Commun. **112**, 321 (1994).

[21] H. He, M. E. J. Friese, N. R. Heckenberg, and H. Rubinsztein-Dunlop, Phys. Rev. Lett. **75**, 826 (1995).

[22] N. B. Simpson, K. Dholakia, L. Allen, and M. J. Padgett, Opt. Lett. **22**, 52 (1997).

[23] M. S. Soskin, V. N. Gorshkov, M. V. Vasnetsov, J. T. Malos, and N. R. Heckenberg, Phys. Rev. A **56**, 4064 (1997).

[24] L. Allen, S. M. Barnett, and M. J. Padgett, *Optical Angular Momentum* (Institute of Physics Publishing, Bristol, 2003); *Optical Tweezers: Methods and Applications*, Series in Optics and Optoelectronics, edited by M. J. Padgett, J. E. Molloy, and D. McGloin (CRC Press, Boca Raton, FL, 2010), and references therein.

[25] L. C. Dávila Romero, D. L. Andrews, and M. Babikar, J. Opt. B **4**, S66 (2002).

[26] X. Cai, J. Wang, M. J. Strain, B. Johnson-Morris, J. Zhu, M. Sorel, J. L. OBrien, M. G. Thompson, and S. Yu, Science **338**, 363 (2012).

[27] M. Babiker, C. R. Bennett, D. L. Andrews, and L. D. Romero, Phys. Rev. Lett. **89**, 143601 (2002).

[28] G. F. Quinteiro and P. I. Tamborenea, Phys. Rev. B **79**, 155450 (2009); G. F. Quinteiro and J. Berakdar, Opt. Express **17**, 20465 (2009).

[29] G. F. Quinteiro, A. O. Lucero, and P. I. Tamborenea, J. Phys. Condens. Matter **22**, 505802 (2010).

[30] G. F. Quinteiro, P. I. Tamborenea, and J. Berakdar, Opt. Express **19**, 26733 (2011).

[31] A. Thakur and J. Berakdar, Opt. Express **18**, 27691 (2010).

[32] A. Picón, A. Benseny, J. Mompart, J. R. V. de Aldana, L. Plaja, G. F. Calvo, and L. Roso, New J. Phys. **12**, 083053 (2010).

[33] M. Babiker, W. L. Power, and L. Allen, Phys. Rev. Lett. **73**, 1239 (1994).

[34] R. Jáuregui, Phys. Rev. A **70**, 033415 (2004).

[35] S. J. van Enk, Quantum Opt. **6**, 445 (1994).

[36] M. Fedorov and M. V. Fedorov, *Atomic and Free Electrons in a Strong Light Field* (World Scientific, Singapore, 1997).

[37] C. Joachain, *Quantum Collision Theory* (North-Holland, Amsterdam, 1975).

[38] J. Hebborn and N. March, Adv. Phys. **19**, 175 (1970).

[39] D. M. Wood and N. W. Ashcroft, Phys. Rev. B **25**, 6255 (1982).

[40] O. Keller and G. Wang, Opt. Commun. **178**, 411 (2000).

[41] O. Keller, Phys. Rep. **411**, 1 (2005).

[42] E. Wells, I. Ben-Itzhak, and R. R. Jones, Phys. Rev. Lett. **93**, 023001 (2004).

[43] A. S. Moskalenko, A. Matos-Abiague, and J. Berakdar, Europhys. Lett. **78**, 57001 (2007); A. Matos-Abiague and J. Berakdar, Phys. Rev. B **70**, 195338 (2004); Phys. Lett. A **330**, 113 (2004).